Local Electrical Characterization of PVDF Textile Filament

Anthony Ferri, François Rault, Antonio Da Costa, Cédric Cochrane, Matthieu Boudriaux, Guillaume Lemort, Christine Campagne, Eric Devaux, Christian Courtois, Rachel Desfeux

Local electrical characterization of PVDF textile filament

Anthony Ferri [1], François Rault [2,*], Antonio Da Costa [1], Cédric Cochrane [2], Matthieu Boudriaux [2], Guillaume Lemort [2], Christine Campagne [2], Eric Devaux [2], Christian Courtois [3], Rachel Desfeux [1]

[1] Univ. Artois, CNRS, Centrale Lille, ENSCL, Univ. Lille, UMR 8181, Unité de Catalyse et Chimie du Solide (UCCS), F-62300 Lens

[2] ENSAIT, GEMTEX – Laboratoire de Génie et Matériaux Textiles, F-59000 Lille

[3] UVHC, LMCPA EA 2443, F-59313 Valenciennes

Correspondence to: F. Rault (E-mail: *francois.rault@ensait.fr*)

ABSTRACT

The piezoelectric behavior of Poly(vinylidene fluoride), PVDF, is known since several decades and is clearly related to its crystalline phases. Many works made on films or fibers have focused on the characterization of the phase transitions during various PVDF processing and on its electromechanical activity by combining several techniques. Piezo-force microscopy (PFM) is an interesting tool to underline the crystalline forms and piezoelectricity efficiency of PVDF at the local scale. However, this technique is little used on samples in the form of fibers and in this case, it is most often nanofibers. In this work, two conventional PVDF textile filaments, with different weak draw ratio, are produced and analyzed by FTIR, XRD and PFM. We demonstrate that the PFM analysis can be relevant for specimens presenting low signals during other characterizations. Therefore, the local piezo-/ferroelectricity into the fiber is highlighted underlining the existence of the polar phases of PVDF. Then, the effective piezoelectric coefficient d33 of PVDF fiber drawn with a ratio of 1.5 is estimated at 12 pm/V.

KEYWORDS: Poly(vinylidene fluoride) PVDF; melt-spun textile fiber; piezoelectric effect; piezo-force microscopy

INTRODUCTION

Over the last decade, textile instrumentation has attracted the attention of several researchers [1]. Firstly confined to specific technical areas and dedicated to well-defined users (e.g. tracking for military [2, 3], sensors for firefighters [4, 5], etc.), this topic increasingly integrates mass-market applications due to the emergence of connected, e-textile or so-called “smart textiles” in various areas such home textiles [6], fashion [7], sport [8, 9], health [10, 11], etc. A better integration of “intelligent functions” in textile structures is particularly relevant in the latter sectors, where monitoring of body parameters is of particular interest. Due to the multiplication of sensors, process unit and communicative system, the need of energy and data of sector is substantial. One of the possible solutions is energy harvesting by textile structure itself [11, 12]. Some solutions based on the conversion of energy (thermal, mechanical, etc.) to electric voltage are nowadays investigated in laboratories.

Piezoelectric materials show reversible relationships between electric charge and mechanical deformation called converse and direct piezoelectric effect [13]. The latter leading to an electric charge generation during mechanical stress can be used in a wide variety of applications from neural stimulation [14, 15], sensors development [16, 17] or energy harvesters [13, 17]. As a consequence, such materials and more particularly piezoelectric polymers are perfect candidates to solve the main problem for e-textiles, i.e.: develop self-sustaining energy sensors. Among the piezoelectric polymers available, fluoropolymers such as poly(vinylidene fluoride) (PVDF) and its copolymers show the better piezoelectric behavior [18]. Although copolymers crystallize in polar form suitable for piezoelectric properties, PVDF is still preferred due to its relative low cost. Nevertheless, depending on the processing conditions it can crystallize in five different structures: α, δ, ε, γ, β [19]. The β phase is the most polar phase [20].

Accordingly, this one is targeted to convert mechanical deformation into electric energy. The development of PVDF textile energy harvesters requires solving many scientific issues such as the generation of the β phase in the fibers but also its evaluation as well as its electromechanical activity.

On one hand, various methods exist to determine the presence of β phase into PVDF. Usually this polar crystalline form is characterized by one or more thermal analysis techniques [21] (differential scanning calorimetry (DSC), modulated DSC [22], dynamic mechanical analysis (DMA) or thermal mechanical analysis (TMA)) as well as X-ray diffraction (XRD) and spectroscopy measurements (FTIR, Raman, NMR) [23]. Depending on the test used, it is easily to evaluate qualitatively and quantitatively the presence of β phase in PVDF fiber. DSC is a fast and controlled characterization method on fiber. However, as in thermal analysis techniques, melting and recrystallization phenomena during the test may disrupt the analysis of the results. Other limitations for easy characterization such as the size, the form and the morphology of produced fibers have to be taken into account in some other tests. Thus, it is often necessary to design special specimen holder for filaments and to consider the orientation of sample during the test [24]. To correlate mechanical stretching and β phase, characterizations can advantageously be made in situ by X-ray [25] or spectroscopy measurements [26]. Nevertheless, to our knowledge only few studies are made in line with real process conditions [27]. Even if FTIR experiment is easiest ex-situ spectroscopy technique available, the presence of relatively close characteristic peaks requires carefully conclusions and to correlate the results with other tests [28]. Furthermore, this technical analysis presents some limitations for specific multilayer materials.

On the other hand, characterization of piezoelectric behavior is essential to improve the design of textile energy harvester and to understand all important phenomena occurring during the processing of PVDF fiber. Numerous varied experimental methods based on direct or converse effect exist to determine piezoelectricity efficiency [29]. Among all these techniques Berlincourt type piezometer is a useful

solution for measuring piezoelectric coefficient on films. On textile fabric however, because of its small deformations, this test only allows soliciting the structure and do not give the piezoelectric response of the fiber. The evaluation of piezoelectric behavior of the textile can be made by output voltage measurements under large deformation using DMA for instance [30]. However, processing such structures is time and material consuming and gives only an average value at the fabric scale. Textile structures can be considered as a multi-scale material and a characterization of the piezoelectric behavior at each scale is relevant. Currently, there is no standardized test at the fiber scale for the measurement of piezoelectric coefficients and for the correlation with the β phase. Piezoelectric force microscopy (PFM) characterization is a relevant technical analysis to locally determine the presence of polar phase in the fiber and to evaluate its piezoelectric coefficient [31, 32]. PFM analyses have been carried out on materials at the dedicated measuring scale of the apparatus, i.e. on nanofibers [33-36]. To our knowledge, only one study has been published on the characterization of a textile filament [37]. However, this monofilament with a diameter around 150 µm is not totally representative of the classical diameters used in textile applications. Indeed, in the work described by Soin *et al.* such large monofilament has been chosen to confer rigidity to the spacer fabric produced [37]. The textile fibers used in the yarns have conventionally diameters of less than 100 µm and consequently a lack of knowledge on electromechanical behavior for such 30 µm diameter fiber is underlined. Thus, the aim of this study is to leverage of PFM analysis for the development of micro-scale PVDF textile fiber by locally probing the physical properties. These first experimental trials on such fibers are particularly interesting. Indeed, they can have important implications for many researchers working on the development of multicomponent piezoelectric fiber systems for energy harvesting where conventional analyses could not be sufficient.

EXPERIMENTAL

Materials

Commercial grade of PVDF was obtained by Solvay (PVDF Solef 1006, Solvay, Belgium). The average melt flow index (MFI) is 40 g/10 min (load of 2.16 kg at 230 °C) and the density is 1780 $kg.m^{-3}$ in the solid state. Before melt spinning, PVDF is dried in oven for 24 h.

Sample preparation

Multifilament yarns were produced using a spinning device Spinboy 1 from Busschaert Engineering. Four successive temperature of the spinning screw extruder are 80, 190, 200, and 210 °C. A volumetric pump ensured the injection of the molten polymer into two parallel dies each containing 40 holes (diameter of 400 mm) with a flow rate of 35 $cm^3.min^{-1}$ in order to obtain a continuous multifilament yarn which was cooled down by air and coated with a surfactant. Finally, the multifilament yarn was hot drawn between two series of rolls. The ratio between rotation speed of the second roll (R2) and the first roll (R1) is called Draw Ratio (DR). Previous study has shown that different DR can be obtained up to a DR of 3 (R1: 150 $m.min^{-1}$ and R2: 450 $m.m^{-1}$) leading to β-phase higher than 50 %. Due to future works and in particular that the development of multicomponent fibers having layers with different behavior under drawing (use of various polymers with or without fillers), a relatively low DR has been chosen for this study.[38] In addition, this low DR seems to be an appropriate strategy to highlight the powerfull of the PFM tool to detect piezo-activity in such textile fiber with relatively low polar phase content.

Characterization

FTIR

A Thermo Scientific FTIR ATR Nicolet Spectrometer was used for recording the infrared spectra of as-spun (DR = 0) and drawn (DR = 1.5) fibers of PVDF. To perform the tests, fibers are lined up on a ZnSe substrat and analyzed in reflection mode. The samples were scanned eight times in the range of 600 to 1500 cm^{-1}.

XRD

XRD measurements were carried out using a PANalytical diffractometer with Bragg-Brentano geometry. The radiation source was Cu Kα with a wavelength of 1.5418 Å. The scan rate was set at 1 second per step of 0.028 (2h).

AFM/PFM

Local characterizations were carried out under environmental conditions with a MFP-3D atomic force microscope from Asylum Research (USA). Surface morphology was characterized in AC mode, while PFM analyses were performed with Pt/Ir conductive tip coating (Nanosensors PPP-EFM probes, k ~2.8 N/m) and ground conductive substrates [39, 40]. Dual AC resonance tracking (DART) PFM was employed to enhance the piezoelectric signal [41]. The PFM probe was calibrated by using the GetReal procedure from Asylum Research, where both inverse optical lever sensitivity (InvOLS) and spring constant of the cantilever are calibrated in one step without touch the surface, then we probed our reference sample ($Pb(Mg_{1/3}Nb_{2/3})O_3$–$PbTiO_3$ thin film) with known d_{33} piezoelectric coefficient.

RESULTS AND DISCUSSION

Charaterization of polar phase by FTIR and XRD

Absorbance spectra recorded during FTIR experiments for PVDF as-spun fiber (DR = 0) and fiber drawn with a ratio of 1.5 and XRD diffraction patterns of the same fibers are shown in figure 1. In the FTIR spectra, the characteristic peaks of the α phase of PVDF at wavenumbers 760, 795, 855 and 976 cm^{-1} can be observed for all both fibers. It can be seen from the spectra that drawn fiber (DR = 1.5) has distinct shoulder and peaks at wavenumbers 1234 and 1279 as well as 840 cm^{-1}. The shoulder suggests the presence of γ-phase while the peaks represent β-phase of PVDF or more generally the polar phase (β/ γ) for this at 840 cm^{-1} [42]. All these results are in agreement with previously reported studies on influence of drawing during the spinning process of PVDF. Stresses applied during the fiber production can transform the α-phase of PVDF into β and/or γ polar phases [22, 38]. Usually XRD patterns are used to confirm the results obtained from FTIR tests. However, in the diffractogram of both fibers (drawn and undrawn) no characteristic diffraction peaks of β (peak at 20.7°) and γ phases are present. The first peaks at 2θ = 17.9° and 2θ = 18.4° corresponds respectively to the (100) and (020) diffraction planes while the last peak at 2θ = 20.1° is linked to the (110) plane. These two conventional analysis techniques show some of their limitations such as a lack of sensitivity and an average analysis of the considered systems. In these cases, the use of specific tools to perform local analyzes can be very relevant.

[Fig. 1 about here]

Charaterization of piezoresponse

For PFM measurements, fibers were directly deposited on conductive disk with carbon paste in-between and the nano-probe tip was scanning individual fiber, as illustrated on figure 2a. Optical image of an individual fiber with 35 µm in diameter is shown on figure 2b, while the characteristic morphology of the fiber is presented in figure 3a, as measured by AFM. No preferential direction is observed for such low draw ratio (DR = 1.5). The nanoscale tip was used as movable top electrode at the surface of the fiber in order to locally probe both the electromechanical activity and the ferroelectric polarization. The out-of-

plane PFM amplitude image shown in figure 3b displays contrasts corresponding to the local deformation of the fiber under electric field. Correspondingly, a strong contrasted out-of-plane PFM phase image is obtained suggesting several orientations for the polarization within the fiber, as seen on figure 3c. The obtained domains present sub-micrometer sizes, which could be correlated by the relatively low content of the β-phase resulting in small crystallites size. Black and white regions can be attributed to the out-of-plane component of the ”upward” and “downward” polarization states, respectively, as related to the negative piezoelectric coefficient of the PVDF polymer. The various contrasts observed on both amplitude and phase PFM images reveal randomly oriented as-grown domains, which can be explained by the non-preferential orientation for polymer chains and crystals in the fiber at low draw ratio [43] correlated by the absence of preferential direction on AFM image. Besides, there is no correspondence between the topographic image (figure 3a) and the PFM signals, indicating that the nature of the contrasted regions is related to the intrinsic electromechanical activity of the fiber and not to the cross-talk with the topography (see figure 3d), to the electrostatic effect or to surface reactions. Therefore, these as-grown domain patterns clearly evidence the local piezo-/ferroelectricity into the fiber, demonstrating the existence of the polar crystalline phase. Besides, it is worth noting that the apparition of electro-active zones is for un-poled polymer fibers, as already observed in such PVDF-based fibers [33-35].

[Fig. 2 about here]

[Fig. 3 about here]

Switching behavior and vibration amplitude were then probed by recording phase and amplitude piezoresponse hysteresis loops, respectively. DC bias voltage applied to the fixed probing tip was swept between ±40 V, i.e. high voltage PFM module was used to switch the polarization since the bulk coercive field of PVDF is known to be large (50 MV/m) [44]. Remnant signal (off-field mode) was measured in order

to eliminate electrostatic effect for the benefit of the electromechanical contribution [45, 46]. The figure 4 exhibits the piezoloops recorded over the free surface of the fiber. A square hysteretic behavior and two stable states of opposite polarization are observed on the phase loop pointing out the ferroelectric nature of the PVDF fiber. Indeed, a near 180° switching is observed for the domain phase under the DC bias voltage (the slight lower phase shift can be due to a small remaining electrostatic contribution). On the same figure is displayed the amplitude loop simultaneously measured showing a typical butterfly-shaped due to the inverse piezoelectric effect with clear saturation for higher applied voltages. These local PFM spectroscopic measurements reinforce the presence of the polar phase which presents ferro- and piezo-electric properties. As a remark, we note a slight asymmetry in switching process, as indicated by the shift of the piezoloops toward negative voltage values. This asymmetry is characteristic of an imprint behavior and point out the existence of an internal built-in electric field in the fiber [47, 48]. The main reason is probably our strong asymmetric configuration, for which the top and bottom electrodes are constituted of Pt-Ir nanometric probe and conductive disk covered with carbon paste respectively, leading to different boundary conditions. We can also note that the shape of the amplitude loop is slightly asymmetric. This asymmetric shape can be also explained by the difference between the work functions of the tip and the bottom electrode, resulting in an internal bias field [49]. From the phase PFM loop, we determine a coercive voltage of 15 V. Considering the fiber diameter of 35 µm, we estimate a coercive field of 430 kV/m. This value is much lower than 50 MV/m in the case of bulk PVDF mentioned above. The difference can be explained by the micrometric size of our fiber which enables to decrease the voltage required to switch the polarization. Indeed, for such electroactive polymers with relatively high coercive field, a possible way to decrease the switching voltage is to synthesize these compounds as thin film form [50]. In addition, the nanometric size for ferroelectric domains seen on the figure 3c can disturb the cooperative coupling among these domains, leading to a decrease of the spontaneous polarization and thus to a reduction of the coercive voltage [51]. Also, such small ferroelectric domains are more efficiently switched

by external electrical bias, leading to narrow hysteresis loops. On the other hand, we have to keep in mind that the physical processes considered for measuring the coercive field are different when using a movable tip at the nanoscale level and planar electrodes at the macroscopic scale. From the amplitude loop, the higher deformation at the maximum bias voltage is about 600 pm, but it is enhanced by the resonance (DART PFM method). In addition, for such polymer material, the loss is considered as pretty high, which leads to a low quality factor Q of around 10 [52-54]. Considering the amplitude A detected by PFM is proportional to $A = d_{33}V_{ac}Q$, [52, 53] and the driving voltage used for the piezoloops measurements was Vac = 5 V, we can estimate the effective piezoelectric coefficient as d_{33} = 12 pm/V (absolute value). This value is lower than others reported for PVDF-based fibers and determined by similar PFM analyses. Indeed, d_{33} coefficient of 30 pm/V was measured for β-phase PVDF fiber, which reaches 35 and 54 pm/V when added by carboxyl functionalized multiwall carbon nanotubes (CNTs) and silver decorated CNTs respectively [55]. M. Kanik *et al.* obtained an effective piezoelectric constant of 58.5 pm/V for γ-PVDF nanoribbons [36] while d_{33} of 45-50 pm/V was determined for $BaTiO_3$/β-PVDF composite fibers [34]. However, for all these studies, the PVDF-based fibers are in the nanometric size range, which can reasonably explain the higher d_{33}, as compared to the microscopic size of our fibers. It is known that nanoscale confinement induces very high piezoelectric response, mainly due to the larger contribution of the domain wall motion in such nanofibers [36, 56-60]. In addition, the β-phase content in our fibers fabricated at DR = 1.5 is not optimized (the β-phase is estimated around 15%) compared to higher DR [38] limiting the piezo-active volume probed by the AFM tip and leading to lower electromechanical activity. However, beyond this value of 12 pm/V, the PFM technique was shown to be suitable to demonstrate the electromechanical response in such individual micrometer-scale PVDF textile filament, evidencing the existence of β and γ polar phases, which is essential in view of fabrication of complex multicomponent fibers.

[Fig. 4 about here]

CONCLUSIONS

As-spun (DR = 0) and drawn (DR = 1.5) fibers of PVDF have been produced by melt spinning process and characterized during FTIR, XRD and PFM experiments. FTIR spectra revealed small intensity peaks than can be attributed to the polar phase of PVDF for samples having a draw ratio at 1.5. Nevertheless, the presence of such crystalline form could not be confirmed by XRD. It seems that the transformation of α into β phase during the spinning process is too low to present a sensitive signal. The feasibility and the interest of PFM analysis on such fiber was investigated as a first step of the development of more complex piezoelectric fiber, *i.e*: multicomponent fiber with concentric layers of different polymers around the PVDF. Different problems such as adhesion between the components will limit the drawability of final fiber and the possible conversion of crystalline phases of PVDF. Thus, it is supposed to obtain weak responses of the piezoelectric behavior of PVDF with conventional analyses. In this context, PFM can be relevant for future development of piezoelectric PVDF textile filament. In this work, PFM analyses have revealed phase and amplitude PFM contrasts for pristine regions over the surface of the fiber without correlation with the associated AFM morphology, which are related to the polar β-phase of the PVDF. From piezoresponse loops, local effective piezoelectric constant of about 12 pm/V was determined, evidencing the electromechanical behavior of the individual fiber at the local scale. These performances are required for considering such micro-scale functional fibers in textile applications.

ACKNOWLEDGEMENTS

This work is carried out under the regional program “Projets Emergents” and in the framework of the project entitled “Development of tricomponent piezoelectric polymer fibers for energy harvesting textiles”. The authors thank the Region Nord-Pas-de-Calais (France) for its financial support, and also gratefully acknowledge Solvay for the supply of PVDF. The “Région Hauts-de-France” and the “Fonds

Européen de Développement Régional (FEDER)" under the "Contrat de Plan État-Région (CPER)" project "Chemistry and Materials for a Sustainable Growth" are also gratefully acknowledged for funding of MFP-3D microscope.

REFERENCES AND NOTES

1. V. Koncar in "Smart Textiles and their Applications", (V. Kocar Ed.), pp. 1–8, Woodhead Publishing, Oxford, 2016. doi: 10.1016/B978-0-08-100574-3.00001-1

2. S. Scataglini, G. Andreoni and J. Gallant, *Proc. 2015 Work Wearable Syst. Appl. Italy*, 53–54 (2015). doi: 10.1145/2753509.2753520

3. R. Nayak, L. Wang and R. Padhye in "Electronic textiles: Smart Fabrics and Wearable Technology", (T. Tilak Ed.), pp. 239–256,Woodhead Publishing, Oxford, 2015. doi: 10.1016/B978-0-08-100201-8.00012-6

4. R. Soukup, T. Blecha, A. Hamacek and J. Reboun*, Proc. of the 5th Electronics System-integration Technology Conference (ESTC) Finland*, 1–5 (2014). doi: 10.1109/ESTC.2014.6962821

5. S. Mandal and G. Song, *Text. Res. J.*, **85**, 101 (2014). doi: 10.1177/0040517514542864

6. P. Brauner, J. van Heek, M. Ziefle,N. Al-huda Hamdan and J. O. Borchers, *Proc. of the 2017 ACM International Conference on Interactive Surfaces and Spaces United Kingdom*, 151–160 (2017). doi: 10.1145/3132271.3134128

7. J. Berzowska, *TEXTILE*, **3**,:58 (2005). doi: 10.2752/147597505778052639

8. B. Zhou, G. Bahle, L. Fürg, M. S. Singh, H. Z. Cruz and P. Lukowicz, *Proc. 2017 IEEE International Conference on Pervasive Computing and Communications Workshops (PerCom Workshops).U.S.A.*, 85–87 (2017). doi: 10.1109/PERCOMW.2017.7917531

9. D. Tama, P. Gomes, M. J. Abreu, A. P. Souto and H. Carvalho, *Proc. XIV Int. Izmir Text. Appar. Symp. Turkey*, (2017)

10. A. Pantelopoulos and N. G. Bourbakis, *IEEE Transactions on Systems, Man, and Cybernetics, Part C (Applications andReviews)*, **40**,:1 (2010). doi: 10.1109/TSMCC.2009.2032660

11. M. Stoppa and A. Chiolerio, *Sensors*, **14**, 11957 (2014). doi: 10.3390/s140711957

12. V. Kaushik, J. Lee, J. Hong, S. Lee, S. Lee, J. Seo, C. Mahata and T. Lee, *Nanomaterials*, **5**, 1493 (2015). doi: 10.3390/nano5031493

13. S. R. Anton and H. A. Sodano, *Smart Materials and Structures*, **16**, R1 (2007). doi: 10.1088/0964-1726/16/3/R01

14. A. Marino, G. G. Genchi, V. Mattoli and G. Ciofani G, *Nano Today*, **14**, 9 (2017). doi: 10.1016/j.nantod.2016.12.005

15. A. Marino, G. G. Genchi, E. Sinibaldi and G. Ciofani, *ACS Appl. Mater. Interfaces*, **9**, 17663 (2017). doi: 10.1021/acsami.7b04323

16. P. Ueberschlag, *Sensor Review*, **21**, 118 (2001). doi: 10.1108/02602280110388315

17. C. Dagdeviren, P. Joe, O. L. Tuzman,K.-II Park, K. J. Lee, Y. Shi, Y. Huang and J. A. Rogers, *Extreme Mechanics Letters*, **9**, 269 (2016). doi: 10.1016/j.eml.2016.05.015

18. K. S. Ramadan, D. Sameoto and S. Evoy, *Smart Materials and Structures*, **23**, (2014). doi: 10.1088/0964-1726/23/3/033001

19. A. J.Lovinger, *Macromolecules*, **15**, 40 (1982). doi: 10.1021/ma00229a008

20. P. Martins, A. C. Lopes and S. Lanceros-Mendez, *Progress in Polymer Science*, **39**, 683 (2014). doi:

10.1016/j.progpolymsci.2013.07.006

21. V. Sencadas, S. Lanceros-Méndez and J. F. Mano, *Thermochimica Acta*, **424**, 201 (2004). doi: 10.1016/J.TCA.2004.06.006

22. W. Steinmann, S. Walter, G. Seide, T. Gries, G. Roth and M. Schubnell, *Journal of Applied Polymer Science*, **120**, 21 (2010). doi: 10.1002/app.33087

23. P. Holstein, U. Scheler and R. K. Harris, *Polymer*, **39**, 4937 (1998). doi: 10.1016/S0032-3861(97)10257-9

24. B. Glauß, W. Steinmann,S. Walter, M. Beckers,G. Seide, T. Gries and G. Roth, *Materials (Basel)*, **6**, 2642 (2013). Doi: 10.3390/ma6072642

25. J. Wu and J. M. Schultz, *Macromolecules*, **33**, 1765 (2000). doi: 10.1021/ma990896w

26. M. T. Riosbaas, K. J.Loh, G. O'Bryan and B. R. Loyola, *Proc. SPIE 9061, Sensors and Smart Structures Technologies for Civil, Mechanical, and Aerospace Systems U.S.A.*, (2014). doi: 10.1117/12.2045430

27. M. G. Veitmann, D. Chapron, S. Bizet, S. Devisme, J. Guilment and P. Chapron, *1st workshop Innovative and Avanced Processing for Polymer*, Lyon, (2017).

28. R. Khajavi and M. Abbasipour in "Industrial Applications for Intelligent Polymers and Coatings", (M. Hosseini and A. S. H. Makhlouf Eds), pp.313–336, Springer International Publishing, Switzerland, 2016. Doi: 10.1007/978-3-319-26893-4_15

29. K. Magniez, A. Krajewski, M. Neuenhofer and R. Helmer, *Journal of Applied Polymer Science*, **129**, (2013). doi: 10.1002/app.39001

30. Institute of Electrical and Electronic Engineers, *IEEE Stand*, 176 (1987).

31. A. Gruverman, O. Auciello and H. Tokumoto, *Annual Review of Materials Science*, **28**, 101 (1998). doi: 10.1146/annurev.matsci.28.1.101

32. N. Balke, I. Bdikin, S. V. Kalinin and A. L. Kholkin, *Journal of the American Ceramic Society*, **92**, 1629 (2009). doi: 10.1111/j.1551-2916.2009.03240.x

33. A. Baji, Y. W. Mai, Q. Li and Y. Liu, *Nanoscale*, **3**, 3068 (2011). doi: 10.1039/C1NR10467E

34. A. Baji, Y. W. Mai, Q. Li and Y. Liu, *Composites Science and Technology*, **71**, 1435 (2011). doi: 10.1016/j.compscitech.2011.05.017

35. V. Sencadas, C. Ribeiro, I. K. Bdikin, A. L. Kholkin and S. Lanceros-Mendez, *Physica status solidi*, **209**, 2605 (2012). doi: 10.1002/pssa.201228136

36. M. Kanik, O. Aktas, H. S. Sen, E. Durgun and M. Bayindir, *ACS Nano*, **8**, 9311 (2014). doi: 10.1021/nn503269b

37. N. Soin, T. H. Shah, S. C. Anand, J. Geng, W. Pornwannachai, P. Mandal, D. Reid, S. Sharma, R. L. Hadimani, D. V. Bayramol and E. Siores, *Energy & Environmental Science*, **7**, 1670 (2014). doi: 10.1039/c3ee43987a

38. M. Boudriaux, F. Rault, C. Cochrane, G. Lemort, C. Campagne, E. Devaux and C. Courtois, *Journal of Applied Polymer Science*, **133**, 43244 (2016). doi: 10.1002/app.43244

39. R. Desfeux, A. Ferri, C. Legrand, L. Maës, A. Da Costa, G. Poullain, R. Bouregba, C. Soyer and D. Rèmiens, *International Journal of Nanotechnolog*y, **5**, 827 (2008). Doi: 10.1504/IJNT.2008.018701

40. T. Carlier, M-H. Chambrier, A. Ferri, S. Estradé, J-F. Blach, G. Martin, B. Meziane, F. Peiro, P.

Roussel, F. Ponchel, D. Rèmiens, A. Cornet and R. Desfeux, *ACS Applied Materials & Interfaces*, **7**, 24409 (2015). doi: 10.1021/acsami.5b01776

41. B. J. Rodriguez, C. Callahan, S. V. Kalinin and R. Proksch, *Nanotechnology*, **18**, 475504(2007). doi: 10.1088/0957-4484/18/47/475504

42. S. Ramasundaram, S.Yoon, K. J. Kim, C. Park, *Journal of Polymer Science Part B: Polymer Physics,* ***46***, 2173 (2008). doi:10.1002/polb.21550.

43. J. Chang, M. Dommer, C. Chang and L. Lin, *Nano Energy*, **1**, 356 (2012). doi: 10.1016/j.nanoen.2012.02.003

44. V. M.Fridkin and S. Ducharme, *Physics of the Solid State*, **43**, 1320 (2001). doi: 10.1134/1.1386472

45. C. Harnagea, A. Pignolet, M. Alexe, D. Hesse and U. Gösele, *Applied Physics A*, **70**, 261 (2000). doi: 10.1007/s003390050045

46. D. Martin, J. Müller, T. Schenk, T. M. Arruda, A. Kumar, E. Strelcov, E. Yurchuk, S. Müller, D. Pohl, U. Schröder, S. V. Kalinin and T. Mikolajick, *Advanced Materials*, **26**, 8198 (2014). doi: 10.1002/adma.201403115

47. C. Lichtensteiger, S. Fernandez-Pena, C. Weymann, P. Zubko and J-M. Triscone, *Nano Letters*, **14**, 4205 (2014). doi: 10.1021/nl404734z

48. A. Gruverman, A. Kholkin, A. Kingon and H.Tokumoto, *Applied Physics Letters*, **78**, 2751 (2001). doi: 10.1063/1.1366644

49. J. Hong, H. W. Song, S. Hong, H. Shn, S. Gu and K. No, *Journal of Applied Physics*, **92**, 7434 (2002). doi: 10.1063/1.1524307

50. A. Venimadhav in ”Advances in Polymer Materials and Technology” (A. Srinivasan and S. Bandyopadhyay Eds.), pp. 439–465. CRC Press Taylor & Francis Group, Boca Raton, 2016.

51. L. Yang, X. Li, E. Allahyarov, P. L. Taylor, Q. M. Zhang and L. Zhu, *Polymer*, **54**, 1709 (2013). doi: 10.1016/J.POLYMER.2013.01.035

52. M. A. McLachlan, D. W. McComb, M. P. Ryan, A. N. Morozovska, E. A. Eliseev, E. A. Payzant, S. Jesse, K. Seal, A. P. Baddorf and S. V. Kalinin, *Advanced Functional Materials*, **21**, 941 (2011). doi: 10.1002/adfm.201002038

53. Y. Liu, D. N. Weiss and J.Li, *ACS Nano*, **4**, 83 (2010). doi: 10.1021/nn901397r

54. Y-Y. Choi, P. Sharma, C. Phatak, D. J. Gosztola, Y. Liu, J. Lee, B. Lee, J. Li, A. Gruverman, S. Ducharme and S. Hong, *ACS Nano*, **9**, 1809 (2015). doi: 10.1021/nn5067232

55. M. Sharma, V. Srinivas, G. Madras and S. Bose, RSC Advances, 6,:6251 (2016). doi: 10.1039/C5RA25671B

56. C. Chang, V. H. Tran, J. Wang, Y-K. Fuh and L. Lin, *Nano Letters*, **10**, 726 (2010). doi: 10.1021/nl9040719

57. L. Persano, C. Dagdeviren, Y. Su, Y. Zhang, S. Girardo, D. Pisignano, Y. Huang and J. A. Rogers, *Nature Communications*, 4, 1610 (2013). doi: 10.1038/ncomms2639

58. V. Cauda, G. Canavese and S. Stassi, *Journal of Applied Polymer Science*, **132**, 41667 (2015). doi: 10.1002/app.41667

59. Y. Calahorra, R. A. Whiter, Q. Jing, V. Narayan and S. Kar-Narayan, *APL Materials*, **4**, 116106 (2016). doi: 10.1063/1.4967752

60. R. A. Whiter, Y. Calahorra, C. Ou and S.Kar-Narayan, *Macromolecular Materials and Engineering*, **301**, 1016 (2016). doi: 10.1002/mame.201600135

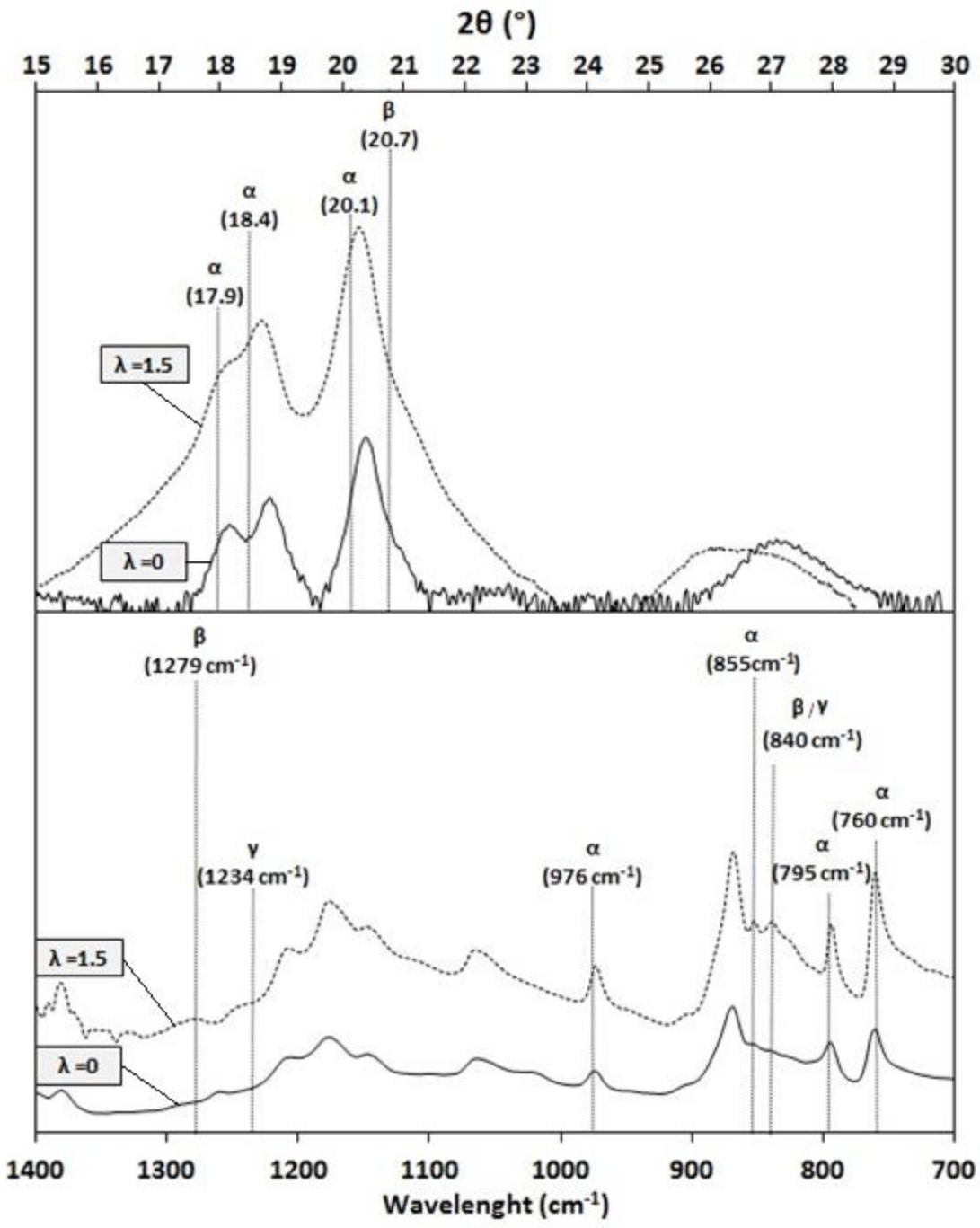

Figure 1. FTIR (bottom) and XRD patterns (up) of as-spun fiber (DR = 0) and fiber drawn with ratio of 1.5.

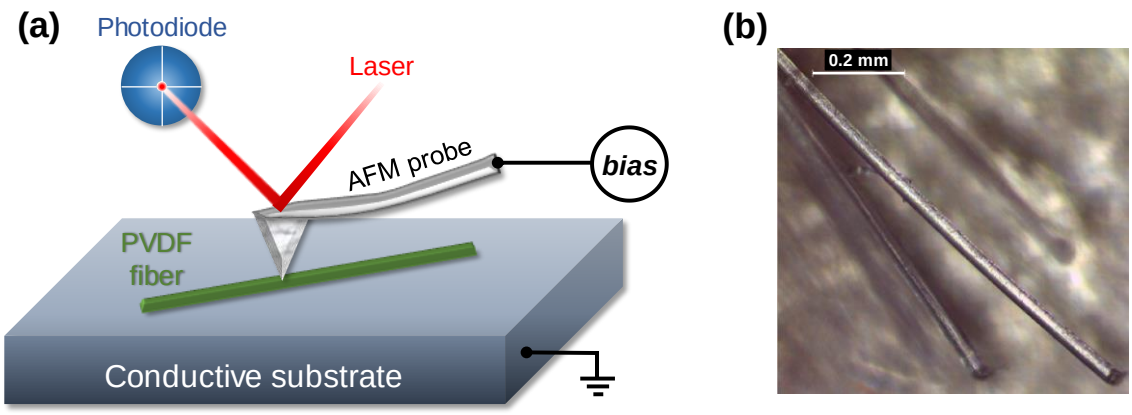

Figure 2. (a) Experimental setup for probing the local electromechanical response of single PVDF fiber (DR = 1.5); (b) optical microscope image of the PVDF fiber of 35 μm in diameter.

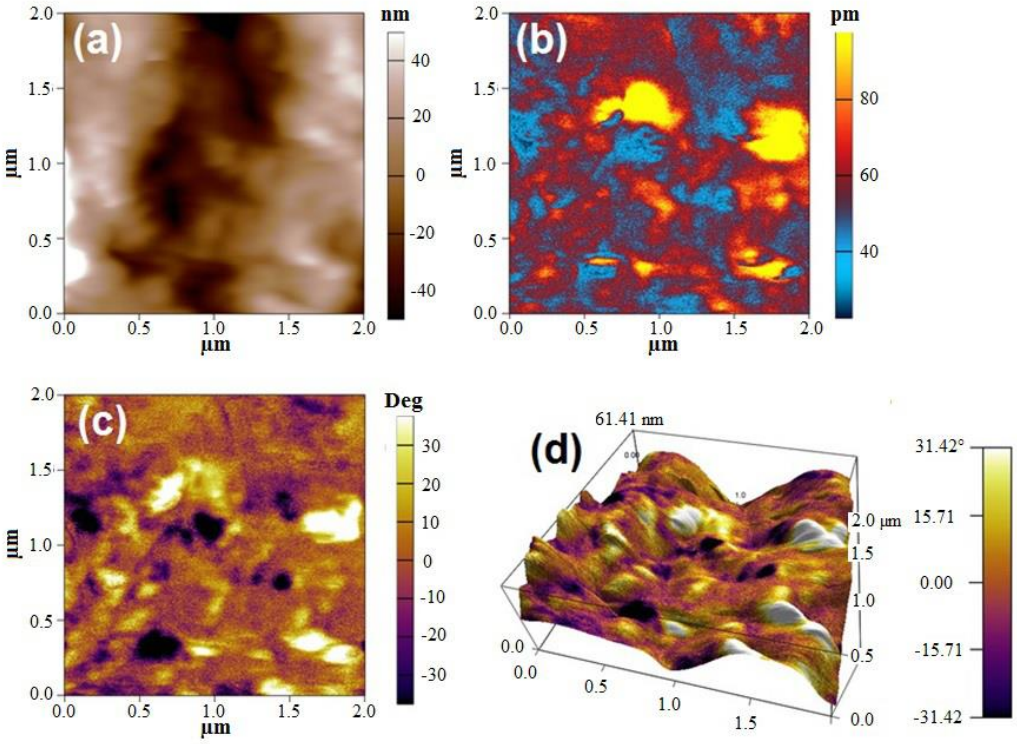

Figure 3. (a) AFM morphology, (b) PFM amplitude and (c) PFM phase images simultaneously recorded on the PVDF fiber. (d) Phase piezoresponse overlaid on top of the 3D topography showing no correlation between the two signals.

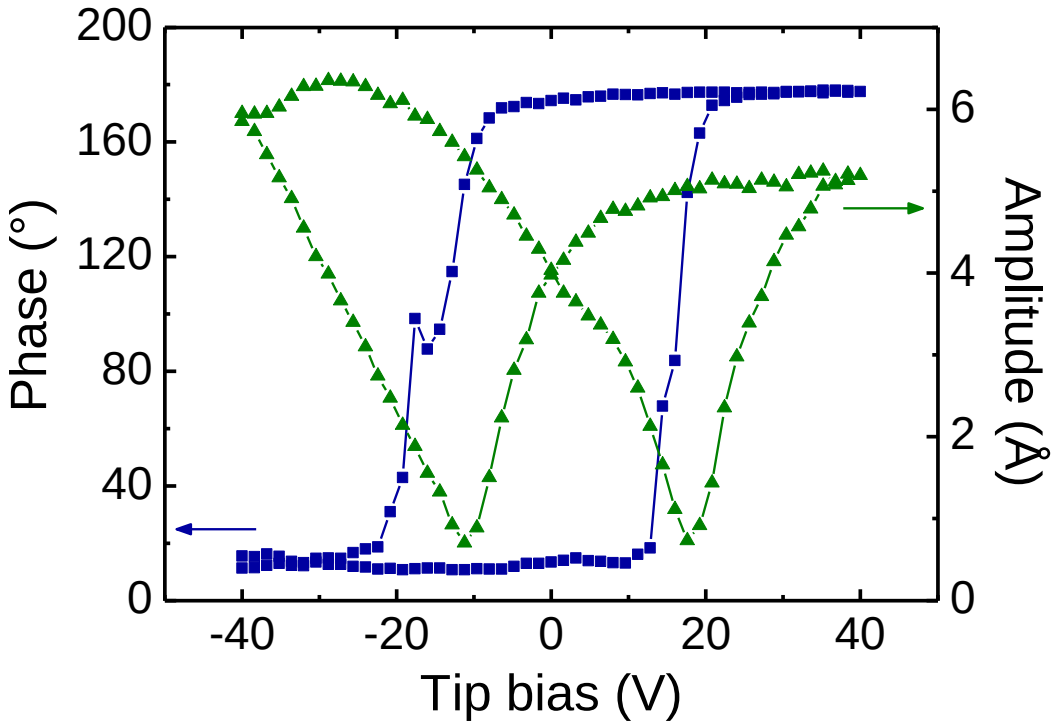

Figure 4. Piezoresponse phase and amplitude loops measured on the PVDF fiber (DR = 1.5).